Available online at www.sciencedirect.com
ScienceDirect
Ceramics International 37 (2011) 1781–1787
CERAMICS INTERNATIONAL
www.elsevier.com/locate/ceramint

Structural and luminescence properties of RE^{3+} (RE = Eu, Tb):$(MgCa)_2Bi_4Ti_5O_{20}$ ceramics

S. Sailaja, B. Sudhakar Reddy *

Department of Physics (Research Centre), S.V. Degree College, Kadapa 516003, India

Received 6 December 2010; received in revised form 10 December 2010; accepted 27 January 2011
Available online 9 March 2011

Abstract

Rare-earth ions (Eu^{3+}, Tb^{3+}) activated magnesium calcium bismuth titanate [$(MgCa)_2Bi_4Ti_5O_{20}$] ceramics were prepared by conventional solid state reaction method for their structural and luminescence properties. By using XRD patterns, the structural properties of ceramic powders have been analyzed. Emission spectrum of Eu^{3+}:$(MgCa)_2Bi_4Ti_5O_{20}$ ceramic powder has shown strong red emission at 615 nm ($^5D_0 \rightarrow {}^7F_2$) with an excitation wavelength λ_{exci} = 393 nm and Tb^{3+}:$(MgCa)_2Bi_4Ti_5O_{20}$ ceramic powder has shown green emission at 542 nm ($^5D_4 \rightarrow {}^7F_5$) with an excitation wavelength λ_{exci} = 376 nm. In addition, from the measurements of scanning electron microscopy (SEM), Fourier transform-infrared (FTIR) and energy dispersive X-ray analysis (EDAX) results the morphology, structure and elemental analysis of these powder ceramics have been studied.

Keywords: B. Grain size; C. Colour; C. Ferroelectric properties; C. Optical properties

1. Introduction

In recent years, a great deal of research has been carried out on the development of high optical quality rare earth (RE) ions doped ceramics. Ceramics are not only having thermal and mechanical properties, but these are also the best host materials to incorporate high concentrations of dopant ions such as rare-earth and transition metal ions and these ceramics can be fabricated at lower cost and in much speedy processes in a large variety of sizes and shapes [1,2]. Rare-earth ion containing materials could perform well in respect of efficient and narrow emissions from them in the visible region [3]. The preparation of ferroelectrics has become an important thing for applications such as memories, pyroelectric detectors, integrated optical modulators, actuators, infrared sensors, display and switching devices [4]. Bismuth titanate is a ferroelectric material and it exhibits useful properties for optical memory, non-volatile memory, piezoelectric and electro-optic devices [5]. Bismuth layer structured ferroelectrics (BLSF) ceramics are useful for piezoelectric device applications because of their high Curie temperatures, low dielectric dissipation factors, low aging rate, high dielectric breakdown strengths, stronger anisotropic electromechanical coupling factors and low temperature coefficients of resonant frequency [6,7]. It is well known that bismuth titanate was found to be more attractive host matrices for rare earth ions because of their low coercive field and high breakdown strength. $(MgCa)_2Bi_4Ti_5O_{20}$ ceramics were conventionally prepared by solid state reaction process, where oxide mixture of Bi_2O_3, TiO_2, $MgCO_3$ and $CaCO_3$ was ball milled, calcinide at an intermediate temperature and finally sintered at high temperature [8]. Rare-earth (RE) ions doped ceramics have attracted much attention in their preparation for their applications involving the production of different visible fluorescent colours such as cathode ray tubes, lamps, X-ray detectors, medical diagnosis, electroluminescence, optical markers, laser materials, phosphors and fluorescent tubes, due to their potential luminescent properties such as high brightness, high efficiency and long working time [9,10]. Among the various RE ions, it is well known that the Eu^{3+} ions show red colour emission ($^5D_0 \rightarrow {}^7F_J$) and Tb^{3+} ions show green colour emission ($^5D_4 \rightarrow {}^7F_J$). Thus the rare earth ions such as $Eu^{3+}$and Tb^{3+} ions give strong luminescence in a variety of lattices and hence it is interesting to study the photo-luminescent properties of $(MgCa)_2Bi_4Ti_5O_{20}$ with these ions.

* Corresponding author. Tel.: +91 8562 244367; fax: +91 8562 259763.
E-mail address: drbsreddyphd@gmail.com (B.S. Reddy).

0272-8842/$36.00
doi:10.1016/j.ceramint.2011.03.005

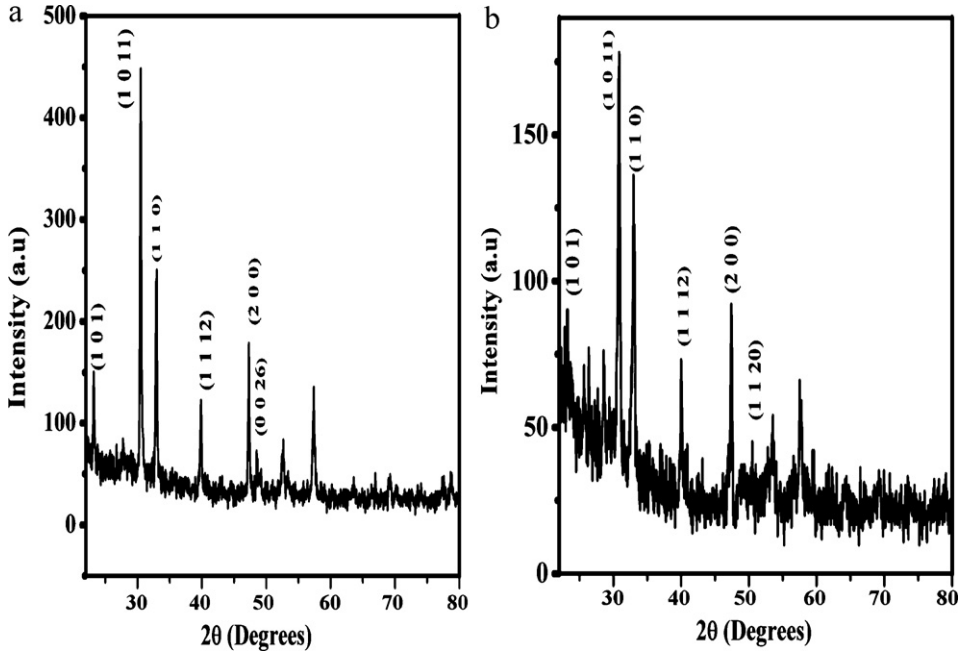

Fig. 1. XRD patterns of (a) $(MgCa)_2Bi_4Ti_5O_{20}:Eu^{3+}$ and (b) $(MgCa)_2Bi_4Ti_5O_{20}:Tb^{3+}$ ceramics.

We have already reported earlier on the spectral analysis of RE^{3+} (Sm^{3+} or Dy^{3+}):$(MgCa)_2Bi_4Ti_5O_{20}$ ceramics [11]. In the present work, we have reported the structural and luminescence properties of couple of rare-earth (0.2 mol% Eu^{3+}, Tb^{3+}) ions doped magnesium calcium bismuth titanate ($(MgCa)_2Bi_4Ti_5O_{20}$) ceramic powders.

2. Experimental studies

Rare-earth ion containing magnesium calcium bismuth titanate ceramics were prepared by heating a mixture with a ratio of 2 mol of magnesium carbonate ($MgCO_3$), 2 mol of calcium carbonate ($CaCO_3$), 2 mol of bismuth oxide (Bi_2O_3), 5 mol of titanium oxide (TiO_2) and 0.2 mol of rare earth oxide (Eu_2O_3, Tb_4O_7) of 99.99% purity in ambient atmosphere. We have adopted the same method to prepare the ceramic powders as described in our earlier paper [11].

Structural characterization of these samples has been carried out from the X-ray powder diffraction measurements on a XRD 3003TT Seifert diffractometer with Cu Kα radiation (λ = 1.5406 Å) at 40 kV and 20 mA and the 2θ range was varied between 20° and 55°. Morphology of the ceramic powder was examined on a ZEISS-EVO-MA15 ESEM. The scanning electron microscopy (SEM) image was obtained for samples by using a 35 m camera attached to a high resolution recording system. The elemental analysis has been carried out by energy dispersive X-ray analysis (EDAX) using an X-ray detector attached to the SEM instrument. The FTIR spectrum (4000–450 cm^{-1}) was recorded on a Perkin Elmer Spectrum1 spectrometer with KBr pellets. Both the excitation and emission

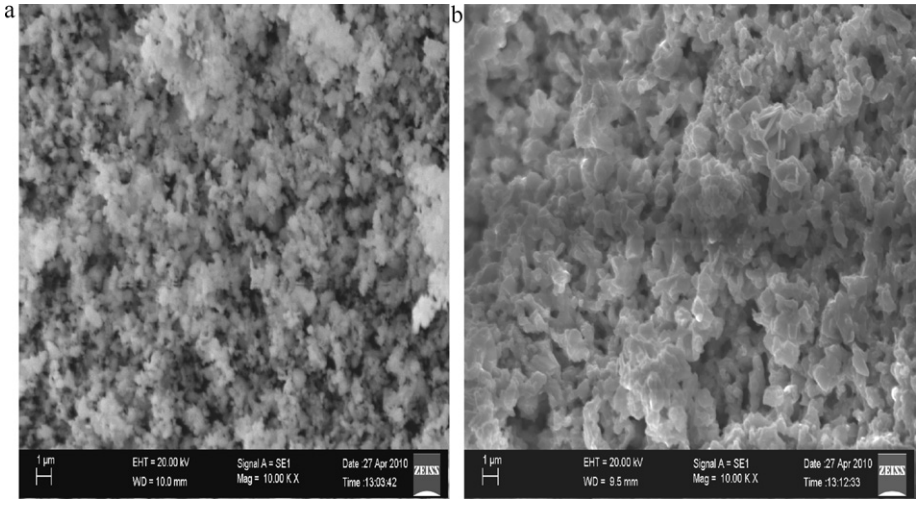

Fig. 2. SEM images of (a) $(MgCa)_2Bi_4Ti_5O_{20}:Eu^{3+}$ and (b) $(MgCa)_2Bi_4Ti_5O_{20}:Tb^{3+}$ ceramic powders.

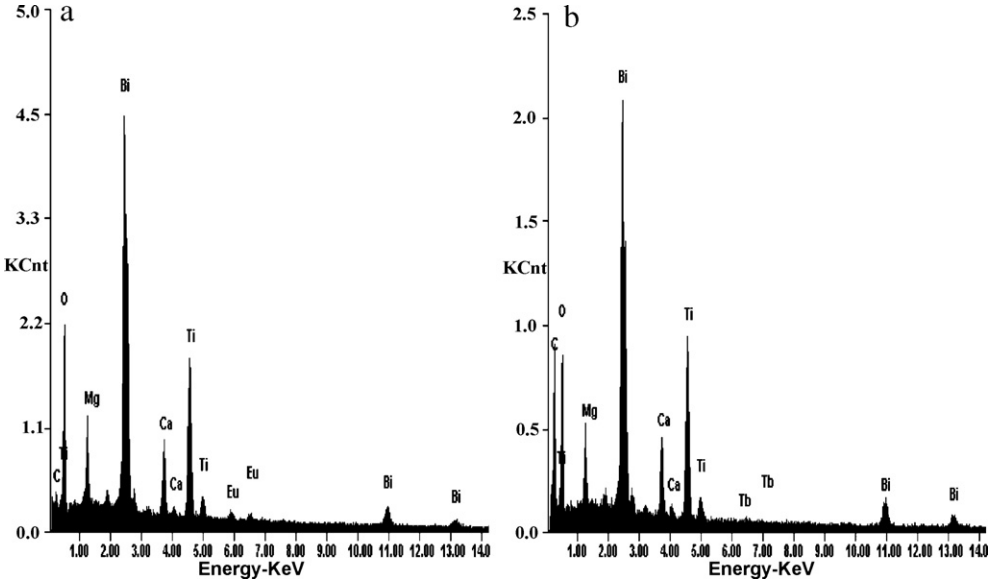

Fig. 3. EDAX images of (a) $(MgCa)_2Bi_4Ti_5O_{20}:Eu^{3+}$ and (b) $(MgCa)_2Bi_4Ti_5O_{20}:Tb^{3+}$ ceramic powders.

spectra were obtained on a SPEX Fluorolog-2 Fluorimeter (Model II) with Data max software to acquire the data with a Xe-arc lamp (150 W) as the excitation source. A Xe-flash lamp with a phosphorimeter attachment was used to measure the lifetimes of the emission transitions of these ceramics.

3. Results and discussion

Fig. 1a and b shows the X-ray diffraction patterns of (0.2 mol%) Eu^{3+} and Tb^{3+}:$(MgCa)_2Bi_4Ti_5O_{20}$ ceramic powders. From these patterns, it is observed that the powders are well crystallized with the peaks corresponding to the tetragonal structure of the standard JCPDS-14-0276. The morphological properties of the obtained ceramic powders were investigated by using the SEM images. Fig. 2a and b shows the SEM micrographs of Eu^{3+} and Tb^{3+}:$(MgCa)_2Bi_4Ti_5O_{20}$ ceramic powders respectively. The obtained images have shown that the particles are agglomerated and the average diameter of the grain size is around at 300–500 nm. To know the presence of rare-earth ions in the ceramics (Eu^{3+} and Tb^{3+}:$(MgCa)_2Bi_4Ti_5O_{20}$) the elemental analysis has been carried out by using the energy dispersive X-ray analysis (EDAX) technique which is

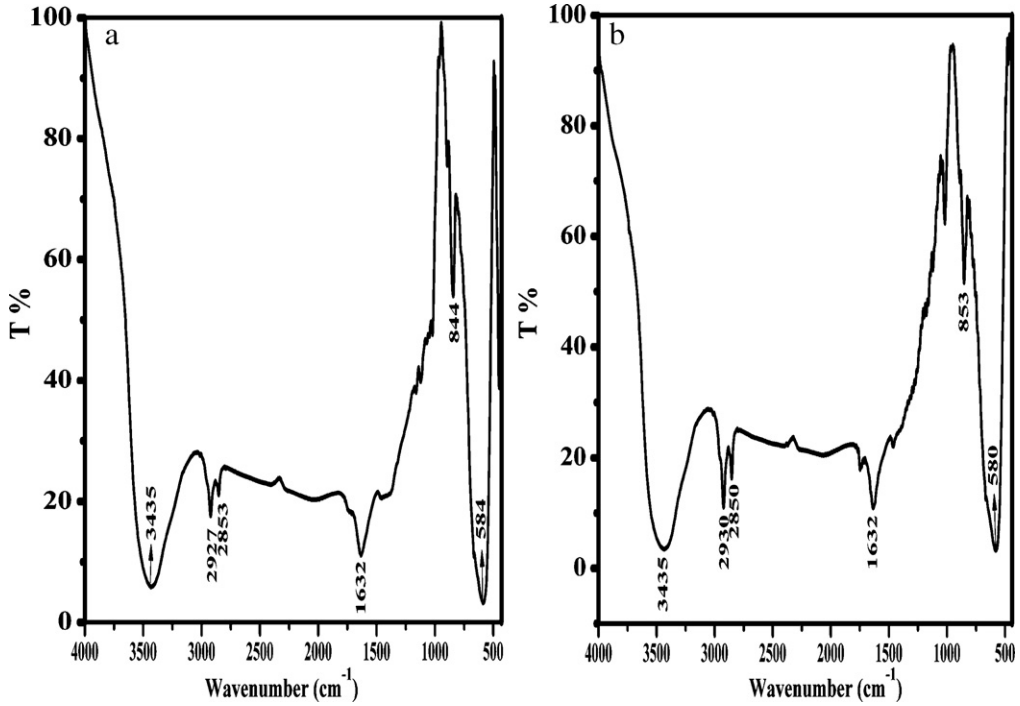

Fig. 4. FTIR spectra of (a) $(MgCa)_2Bi_4Ti_5O_{20}:Eu^{3+}$ and (b) $(MgCa)_2Bi_4Ti_5O_{20}:Tb^{3+}$ ceramic powders.

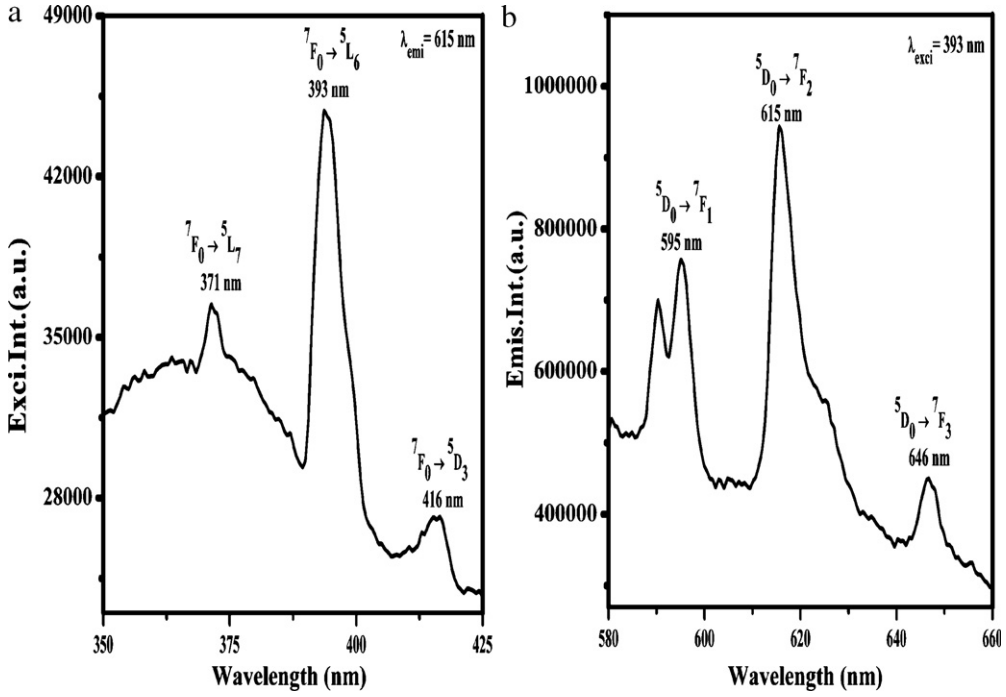

Fig. 5. (a) Excitation spectrum and (b) emission spectrum of Eu^{3+} activated $(MgCa)_2Bi_4Ti_5O_{20}$ ceramic powder.

attached to the SEM system and the measured patterns are shown in Fig. 3a and b, which confirms their presence. The FTIR spectra of Eu^{3+} and Tb^{3+}:$(MgCa)_2Bi_4Ti_5O_{20}$ ceramics are shown in Fig. 4a and b. The FTIR spectra shows the absorption bands in the range 2700–3800 cm^{-1} with absorption band centered at 3435 cm^{-1} which is assigned to the stretching mode of OH groups and a band at 1632 cm^{-1} corresponds to the bending vibrations of H_2O groups. The region 450–1300 cm^{-1} shows the stretching and bending modes of bismuth or titanium bonds.

The excitation spectrum of Eu^{3+}:$(MgCa)_2Bi_4Ti_5O_{20}$ powder ceramic is shown in Fig. 5a. From the measured excitation spectrum, three excitation bands at 371 nm, 393 nm and 416 nm are observed and are assigned to the electronic transitions $^7F_0 \rightarrow {}^5L_7$, $^7F_0 \rightarrow {}^5L_6$ and $^7F_0 \rightarrow {}^5D_3$ respectively. Only the prominent excitation band at 393 nm has been chosen

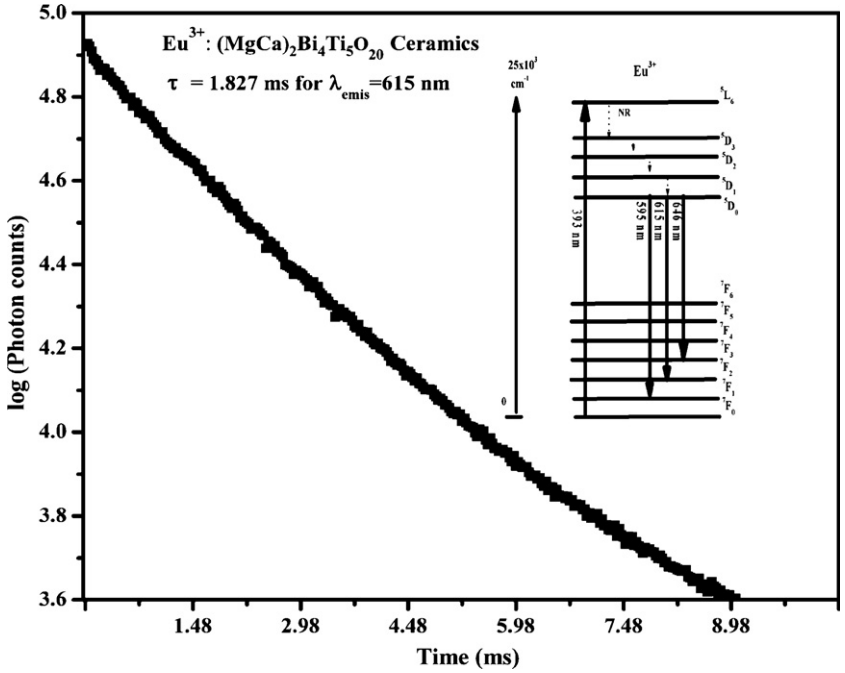

Fig. 6. Decay curve of the emission transition and inset shows energy level diagram of Eu^{3+} activated $(MgCa)_2Bi_4Ti_5O_{20}$ ceramic powder.

for the measurement of emission spectrum of Eu^{3+}:$(MgCa)_2Bi_4Ti_5O_{20}$ ceramic powder. The emission spectrum of Eu^{3+}:$(MgCa)_2Bi_4Ti_5O_{20}$ powder ceramic is shown in Fig. 5b. The emission spectrum of $(MgCa)_2Bi_4Ti_5O_{20}$:Eu^{3+} consists of different spectral lines mainly located in the wavelength range from 580 to 660 nm. These lines correspond to transitions from the excited state $^5D_0$ to the ground state ^7F_J (J = 1–3) of the $4f^6$ configuration of Eu^{3+} and the strongest emission is the electric dipole transition $^5D_0 \rightarrow {}^7F_2$ which peaks at 615 nm when excited at 393 nm. The luminescence spectrum of Eu^{3+}:$(Mg Ca)_2Bi_4Ti_50_{20}$ ceramics consists the transitions only from $^5D_0$ to ^7F_J states. Luminescence from higher excited states such as $^5D_1$ is not observed, indicating very efficient non-radiative relaxation to $^5D_0$ states because of the presence of residual OH groups [12]. The red emission was observed from the Eu^{3+} doped $(MgCa)_2Bi_4Ti_5O_{20}$ ceramic powder under an UV source also. The three emission bands at 595 nm, 615 nm and 646 nm are assigned to the transitions $^5D_0 \rightarrow {}^7F_1$, $^5D_0 \rightarrow {}^7F_2$ and $^5D_0 \rightarrow {}^7F_3$ respectively [13]. Luminescence originating from transitions between 4f levels is predominant due to electric dipole or magnetic dipole interactions [14]. The $^5D_0 \rightarrow {}^7F_1$ transition is purely magnetic dipole allowed and is usually taken as a reference transition because the crystal field does not considerably alter the intensity of this transition. The forced electric dipole $^5D_0 \rightarrow {}^7F_2$ transition is strongly hypersensitive to the environment of Eu^{3+} ions [15]. If Eu^{3+} occupies an inversion symmetry site in the lattice, the orange-red emission and the magnetic dipole transition $^5D_0 \rightarrow {}^7F_1$ (around 590–596 nm) is the dominant transition. On the other hand, if Eu^{3+} does not occupy the inversion symmetry site, the electric dipole transition $^5D_0 \rightarrow {}^7F_2$ (610–620 nm) becomes the dominant transition. From Fig. 5b, the strong red emission is at 615 nm indicating that the electric dipole transition $^5D_0 \rightarrow {}^7F_2$ is the dominant in the measured spectrum. This implies that site of Bi^{3+} occupied by Eu^{3+} ion is not at an inversion center. From this mechanism it is observed that the luminescence performance of activator ions depends on the symmetry site occupied by the activator ions.. From the luminescence spectrum of Eu^{3+}:$(Mg Ca)_2Bi_4Ti_50_{20}$ ceramics it is also observed that $^5D_0 \rightarrow {}^7F_1$ emission band split into two Stark components. This should correspond to tetragonal site symmetry in a crystalline structure with a high degree of disorder [16]. This depends on the site symmetry of the Eu^{3+} ions in the crystalline structure. In other words it is concluded that, the local environment of the rare earth ion plays an effective role on the luminescence performance. The decay curve of the emission band at 615 nm of Eu^{3+}:$(MgCa)_2Bi_4Ti_5O_{20}$ ceramic powder along with its lifetime is shown in Fig. 6. The decay curve for Eu^{3+} emission can be fitted to single exponential function as: $I = K\exp(-t/\tau)$ where 'K' is the constant and value of 'τ' is decay time of Eu^{3+}. The obtained lifetime for Eu^{3+}:$(MgCa)_2Bi_4Ti_5O_{20}$ ceramic powder is 1.827 ms. Inset of Fig. 6 shows the energy level diagram of Eu^{3+}:$(MgCa)_2Bi_4Ti_5O_{20}$ ceramic powder.

The excitation spectrum of Tb^{3+}:$(MgCa)_2Bi_4Ti_5O_{20}$ ceramic powder is shown in Fig. 7a. It indicates three excitation peaks at 350 nm ($^7F_6 \rightarrow {}^5D_2$), 368 nm ($^7F_6 \rightarrow {}^5L_{10}$) and 376 nm ($^7F_6 \rightarrow {}^5G_6$) respectively. Only the prominent excitation band at 376 nm has been chosen for the measurement of emission spectrum of Tb^{3+}:$(MgCa)_2Bi_4Ti_5O_{20}$ ceramic powder. The emission spectrum of Tb^{3+}:$(MgCa)_2Bi_4Ti_5O_{20}$ ceramics with λ_{exci} = 376 nm is shown in Fig. 7b. It is well known that Tb^{3+} have four main emission bands corresponding to the $^5D_4 \rightarrow {}^7F_J$ transitions where J = 3–6. From the emission spectrum, no emission from the $^5D_3$ state is observed because in water the luminescence from the $^5D_3$ state is quenched by fast non-

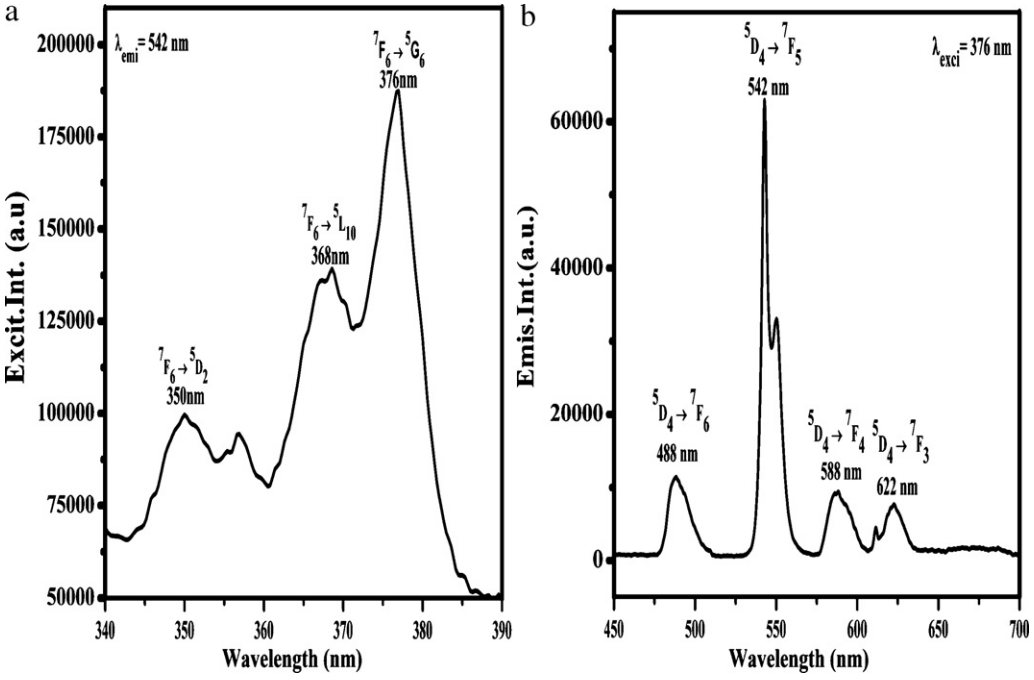

Fig. 7. (a) Excitation spectrum and (b) emission spectrum of Tb^{3+} activated $(MgCa)_2Bi_4Ti_5O_{20}$ ceramic powder.

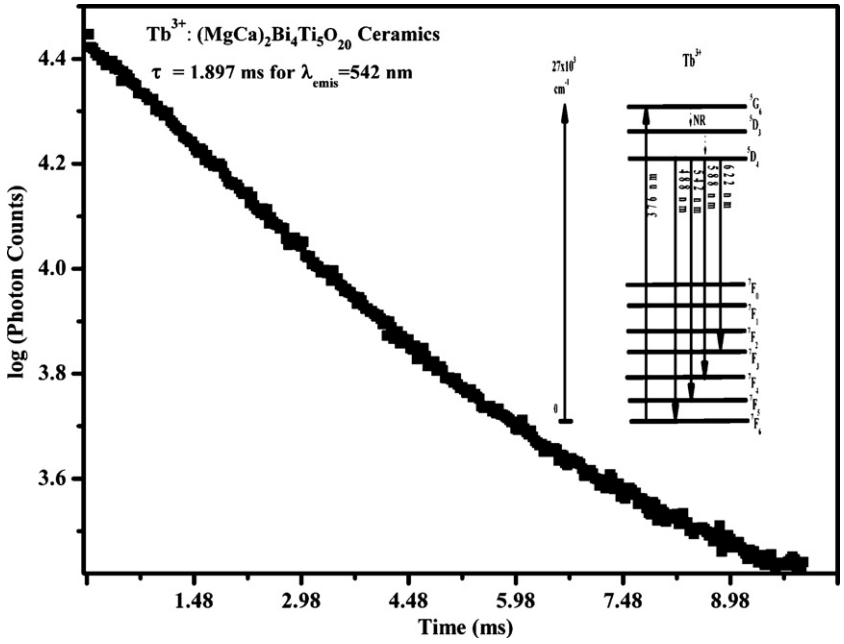

Fig. 8. Decay curve of the emission transition and inset shows energy level diagram of Tb^{3+} activated $(MgCa)_2Bi_4Ti_5O_{20}$ ceramic powder.

radiative relaxation to the $^5D_4$ state, induced by the OH stretching vibrations. Further the luminescence from the $^5D_3$ state is only observed in densified samples, where the OH content is very low [17]. In the present work, the prepared samples are having high OH content due to this, the emission spectrum of Tb^{3+}:$(MgCa)_2Bi_4Ti_5O_{20}$ ceramics consists of the transitions from $^5D_4$ states only. The strongest transition occurred at 542 nm, which is characteristic of the green luminescence of Tb^{3+}. The most dominant peak at 542 nm arises from the $^5D_4 \rightarrow {}^7F_5$ transition, while the other peaks at 488, 588, and 622 nm corresponds to the transitions $^5D_4 \rightarrow {}^7F_6$, $^5D_4 \rightarrow {}^7F_4$, and $^5D_4 \rightarrow {}^7F_3$ respectively [18]. The decay curve of the emission band at 542 nm of Tb^{3+}:$(MgCa)_2Bi_4Ti_5O_{20}$ ceramic powder along with its lifetime is shown in Fig. 8. The decay curve for Tb^{3+} emission can be fitted to single exponential function as: $I = K\exp(-t/\tau)$ where 'K' is the constant and value of 'τ' is decay time of Tb^{3+}. The obtained lifetime for Tb^{3+}:$(MgCa)_2Bi_4Ti_5O_{20}$ ceramic powder is 1.897 ms. Inset of Fig. 8 shows the energy level diagram of Tb^{3+}:$(MgCa)_2Bi_4Ti_5O_{20}$ ceramic powder.

4. Conclusions

In summary it is concluded that, rare-earth (Eu^{3+} and Tb^{3+}) ions activated $(MgCa)_2Bi_4Ti_5O_{20}$ ceramic powders have been synthesized by using a solid state reaction method. From the XRD profiles tetragonal structure of the ceramic powders has been observed. The morphology of the ceramic powders has been studied by using the SEM images, which shows that the particles are agglomerated. Photoluminescence spectrum of Eu^{3+}:$(MgCa)_2Bi_4Ti_5O_{20}$ ceramic has shown a strong red emission and Tb^{3+}:$(MgCa)_2Bi_4Ti_5O_{20}$ ceramic has exhibited an intense green emission. Based on the emission spectral results, we could suggest that these ceramic powders are brightly luminescent and are used as novel optical materials.

References

[1] V. Lupei, A. Lupei, A. Ikesue, Transparent Nd and (Nd, Yb)-doped Sc_2O_3 ceramics as potential new laser materials, Appl. Phys. Lett. 86 (2005) 111–118.
[2] D. Mohr, S.S. Andrea, de Camargo, J.F. Schneider, T.B. Queiroz, H. Eckert, E.R. Botero, D. Garcia, J.A. Eiras, Solid state NMR as a new approach for the structural characterization of rare-earth doped lead lanthanum zirconate titanate laser ceramics, Solid State Sci. 10 (2008) 1401–1407.
[3] K.M. Lin, C.C. Lin, C.Y. Hsiao, Y.Y. Li, Synthesis of $Gd_2Ti_2O_7$:Eu^{3+},V^{4+} phosphors by sol–gel process and its luminescent properties, J. Lumin. 127 (2007) 561–567.
[4] P.C. Joshi, S.B. Krupanidhi, Structural and electrical studies on rapid thermally processed ferroelectronic $Bi_4Ti_3O_{12}$ thin films by metallo-organic solution deposition, J. Appl. Phys. 72 (12) (1992) 5827–5833.
[5] M. Villegas, C. Moure, J.F. Fernandez, P. Duran, Preparation and sintering behaviour of submicronic $Bi_4Ti_3O_{12}$ powders, J. Mater. Sci. 31 (1996) 949–955.
[6] T. Takeuchi, T. Tani, Y. Saito, Unidirectionally textured $CaBi_4Ti_4O_{15}$ ceramics by the reactive templated grain growth with an extrusion, Jpn J. Appl. Phys. Part 1 39 (9B) (2000) 5577–5580.
[7] J.P. Mercurio, A. Souirti, M. Manier, Phase transitions and dielectric properties in some compounds with bismuth oxide layer structure, Mater. Res. Bull. 27 (1) (1992) 123–128.
[8] X.U. Zhijun, R. Chu, Y. Zhang, Q. Chen, L. Zhao, G. Li, Q. Yin, Study on high temperature performances for bismuth layer structured $(Sr_{1-x}Ca_x)_2Bi_4Ti_5O_{18}(0 \leq x \leq 1)$ ceramics, J. Alloys Compd. 487 (2009) 585–590.
[9] B. Yan, X.Q. Su, $LuVO_4$:RE^{3+} (RE = Sm, Eu, Dy, and Er) phosphors by in-situ chemical precipitation construction of hybrid precursors, Opt. Mater. 29 (2007) 547–551.
[10] V.S. Sastri, J.C. Biinzli, V.R. Rao, G.V.S. Rayudu, J.R. Perumareddi, Modern Aspects of Rare Earths and their Complexes, Elsevier, Amsterdam, 2003.

[11] S. Sailaja, B. Sudhakar Reddy, Spectral analysis of RE^{3+} (Sm^{3+} or Dy^{3+}):$(Mg-Ca)_2Bi_4Ti_5O_{20}$ ceramics, Ferroelectrics Lett. Sec. 37 (4) (2010) 1–9.

[12] R. Campostrini, G. Carturan, M. Ferrari, M. Montagna, O. Pilla, Luminescence of Eu^{3+} ions during thermal densification of SiO_2 gel, J. Mater. Res. 7 (1992) 745–753.

[13] J. Fu, Q. Zhang, Y. Li, H. Wang, Highly luminescent red light phosphor $CaTiO_3$:Eu^{3+} under near-ultraviolet excitation, J. Lumin. 130 (2010) 231–235.

[14] G.M. Cai, F. Zheng, D.Q. Yi, Z.P. Jin, X.L. Chen, New promising phosphors $Ba_3InB_9O_{18}$ activated by Eu^{3+}/Tb^{3+}, J. Lumin. 130 (2010) 910–916.

[15] H. Yang, J. Shi, M. Gong, H. Liang, A novel red phosphor: Ca_2GeO_4:Eu^{3+}, J. Rare Earths 28 (4) (2010) 519–522.

[16] A. Bouajaj, M. Ferrari, M. Montagna, Crystallization of silica xerogels: a study by Raman and fluorescence spectroscopy, J. Sol–Gel Sci. Technol. 8 (1997) 391–395.

[17] G. Pucker, S. Parolin, E. Moser, M. Montagna, M. Ferrari, L. Oel Longo, Raman and luminescence study of Tb^{3+} doped monolithic silica xerogels, Spectrochim. Acta A 54 (1998) 2133.

[18] F. Wang, B. Yang, J. Zhang, Y. Dai, W. Ma, Highly enhanced luminescence of Tb^{3+}-activated gadolinium oxysulfide phosphor by doping with Zn^{2+} ions, J. Lumin. 130 (2010) 473–477.